REPORT DOCUMENTATION PAGE

Form Approved OMB NO. 0704-0188

1. REPORT DATE (DD-MM-YYYY)	2. REPORT TYPE	3. DATES COVERED (From - To)
	New Reprint	-

4. TITLE AND SUBTITLE

Refractive index of III-metal-polar and N-polar AlGaN waveguides grown by metal organic chemical vapor deposition

5a. CONTRACT NUMBER

5b. GRANT NUMBER

W911NF-04-D-0003

5c. PROGRAM ELEMENT NUMBER

611102

6. AUTHORS

Martin Rigler, Marko Zgonik, Marc Hoffmann, Ronny Kirste, Milena Bobea, Ramon Collazo, Zlatko Sitar, Seiji Mita, Michael Gerhold

5d. PROJECT NUMBER

5e. TASK NUMBER

5f. WORK UNIT NUMBER

7. PERFORMING ORGANIZATION NAMES AND ADDRESSES

North Carolina State University
Research Administration
2701 Sullivan Drive, Suite 240
Raleigh, NC 27695 -7514

8. PERFORMING ORGANIZATION REPORT NUMBER

9. SPONSORING/MONITORING AGENCY NAME(S) AND ADDRESS(ES)

U.S. Army Research Office
P.O. Box 12211
Research Triangle Park, NC 27709-2211

10. SPONSOR/MONITOR'S ACRONYM(S)

ARO

11. SPONSOR/MONITOR'S REPORT NUMBER(S)

57365-EL-SR.3

12. DISTRIBUTION AVAILIBILITY STATEMENT

Approved for public release; distribution is unlimited.

13. SUPPLEMENTARY NOTES

The views, opinions and/or findings contained in this report are those of the author(s) and should not contrued as an official Department of the Army position, policy or decision, unless so designated by other documentation.

14. ABSTRACT

Optical waveguides of III-metal-polar and N-polar AlGaN are grown on sapphire substrates in order to test their use in integrated optics. The dispersion of the ordinary and extraordinary indices of refraction for films with aluminum mole fraction between 0.0 and 0.30 at four discrete wavelengths has been determined by the prism coupling method. The wavelength dependence of the refractive indices is described well by the first-order Sellmeier dispersion formula. The measurements show a

15. SUBJECT TERMS

AlGaN, refractive index, III-metal polar, N-polar

16. SECURITY CLASSIFICATION OF:			17. LIMITATION OF ABSTRACT	15. NUMBER OF PAGES	19a. NAME OF RESPONSIBLE PERSON
a. REPORT	b. ABSTRACT	c. THIS PAGE			Michael Gerhold
UU	UU	UU	UU		19b. TELEPHONE NUMBER: 919-549-4357

Report Title

Refractive index of III-metal-polar and N-polar AlGaN waveguides grown by metal organic chemical vapor deposition

ABSTRACT

Optical waveguides of III-metal-polar and N-polar AlGaN are grown on sapphire substrates in order to test their use in integrated optics. The dispersion of the ordinary and extraordinary indices of refraction for films with aluminum mole fraction between 0.0 and 0.30 at four discrete wavelengths has been determined by the prism coupling method. The wavelength dependence of the refractive indices is described well by the first-order Sellmeier dispersion formula. The measurements show a small difference in the refractive indices between the two polarities, which is more pronounced at longer wavelengths.VC 2013 American Institute of Physics.

REPORT DOCUMENTATION PAGE (SF298)
(Continuation Sheet)

Continuation for Block 13

ARO Report Number 57365.3-EL-SR
Refractive index of III-metal-polar and N-polar A ...

Block 13: Supplementary Note

Approved for public release; distribution is unlimited.

Refractive index of III-metal-polar and N-polar AlGaN waveguides grown by metal organic chemical vapor deposition

Martin Rigler,[1,a)] Marko Zgonik,[1] Marc P. Hoffmann,[2] Ronny Kirste,[2] Milena Bobea,[2] Ramón Collazo,[2] Zlatko Sitar,[2] Seiji Mita,[3] and Michael Gerhold[4]
[1]*Faculty of Mathematics and Physics, University of Ljubljana, Jadranska 19, 1000 Ljubljana, Slovenia and J. Stefan Institute, Jamova 39, 1000 Ljubljana, Slovenia*
[2]*Material Science and Engineering Department, North Carolina State University, 1001 Capability Drive Raleigh, North Carolina 27606, USA*
[3]*HexaTech, Inc., 991 Aviation Pkwy., Suite 800, Morrisville, North Carolina 27560, USA*
[4]*Engineering Science Directorate, Army Research Office, P.O. BOX 12211, Research Triangle Park, North Carolina 27703, USA*

(Received 31 January 2013; accepted 23 March 2013; published online 3 June 2013)

Optical waveguides of III-metal-polar and N-polar AlGaN are grown on sapphire substrates in order to test their use in integrated optics. The dispersion of the ordinary and extraordinary indices of refraction for films with aluminum mole fraction between 0.0 and 0.30 at four discrete wavelengths has been determined by the prism coupling method. The wavelength dependence of the refractive indices is described well by the first-order Sellmeier dispersion formula. The measurements show a small difference in the refractive indices between the two polarities, which is more pronounced at longer wavelengths. © *2013 American Institute of Physics*. [http://dx.doi.org/10.1063/1.4800554]

AlGaN grown by metalorganic chemical vapor deposition (MOCVD) has a great potential for optoelectronic devices emitting and detecting light in the ultraviolet (UV) wavelength regime. Possible applications for UV light-emitting diodes (LEDs) and lasers could be in the field of water sterilization, bio-agent detection and analysis, solid-state lightning, short-range covert communications, and lithography. There is a strong desire to substitute large inefficient and often toxic mercury lamps by the more reliable and compact solid state based devices. While there are some reports on the fabrication of AlGaN based LEDs in the UV region, only very limited information about direct emitting AlGaN semiconductor lasers is available.[1–9] Most of the problems that evolve during the fabrication of AlGaN based UV laser diodes may be accounted by the deep Si-donor and Mg-acceptor levels, high strain fields and dislocation densities due to large lattice mismatch between the substrate and active layers, as well as poor ohmic contacts for the p- and n-layers.[10–13]

A possible approach to avoid these issues is the second harmonic generation (SHG) of laser light. Typical birefringent materials used for SHG are barium borate (BBO) or lithium triborate (LBO). However, generating second harmonic light using these materials has its disadvantages since large crystals and high excitation laser power are needed; this makes the devices expensive, inefficient, and large. In addition, for most birefringent materials, phase matching in the deep-UV region ($\lambda < 220$ nm) is not attainable.

An alternative to the traditional birefringent materials is the wide bandgap semiconductor AlGaN. This semiconductor belongs to the 6 mm point group, and thus, has five non-zero nonlinear optical coefficients where only two independent components d_{31} and the largest d_{33} need to be considered. The nonlinear optical coefficients d_{33} of AlN, GaN, and AlGaN epitaxial films have been studied theoretically[14] and experimentally.[15–17] Measured nonlinear optical coefficients of AlN and GaN have different values; they depend on the film crystalline structure and the measurement method. The published values of the nonlinear optical coefficients of AlN range from a theoretical estimate of 3.8 pm/V[14] to a measured value of 12.0 pm/V.[17] Respectively, the measured values of the nonlinear optical coefficients of GaN range from 7.4 pm/V to 20.6 pm/V,[15] while theoretically, it has been estimated at 6.0 pm/V.[14]

Since the transparency window of GaN ranges from 13.6 μm to 365 nm, while AlN remains transparent down to 200 nm, AlGaN alloys can be used for photonic devices from the far IR to the deep UV spectral region.[18,19] Unfortunately, conventional phase matching techniques cannot be used in AlGaN thin films; however, quasi phase matching (QPM) is possible.[20–22] Therefore, a periodically modulated nonlinear structure is needed, which alternates the sign of the nonlinear coefficient in regular intervals and corrects for the relative phase mismatch between the fundamental and the frequency doubled light without matching the phase velocities.[23] In contrast to $LiNbO_3$, in AlGaN this periodic change of the sign of the nonlinear coefficients can be achieved during growth (periodically oriented AlGaN).[24] The refractive index and its dispersion determine the QPM structure periodicity for a particular wavelength. In order to design and grow these structures and calculate achievable conversion efficiencies, an exact knowledge of the refractive index for both polarities of AlGaN over a wide compositional range is needed. In addition, a possible difference in the refractive indices between III-metal-polar and N-polar AlGaN would cause reflection losses at every interface between the domains of opposite polarity, which would drastically reduce the conversion efficiency of the SHG structure. As the two different polar surfaces incorporate point defects at a different rate during growth,[25,26] the refractive index at the wavelengths of interest may be different for the two polar domains.

a)Electronic mail: martin.rigler@fmf.uni-lj.si

In this work, the ordinary and extraordinary refractive indices of III-polar and N-polar $Al_xGa_{1-x}N$ ($0 < x < 0.30$) grown by MOCVD on sapphire substrates are determined using the prism coupling technique. It is found that Sellmeier equations can be used to fit the energy dependence of the refractive index over a very broad wavelength range. Furthermore, a slight difference between the refractive indices of III-polar and N-polar $Al_xGa_{1-x}N$ is found, especially for longer wavelengths.

III-metal-polar AlGaN films were grown heteroepitaxially on a 20 nm thick low-temperature (650 °C) AlN nucleation layer on (0001) sapphire using a MOCVD reactor at a growth temperature of 1040 °C, a V/III ratio of 100, and a reactor pressure of 20 Torr.[27] The above V/III ratio was attained by flowing 134 μmol/min of trimethylgallium and 0.3 slm of ammonia with a total flow rate of 7.4 slm using nitrogen diluent gas. The trimethylaluminium molar flow rate was adjusted between 0.0 and 0.17 μmol/min resulting in $Al_xGa_{1-x}N$ films with $0 < x < 0.26$. The N-polar films were grown by applying the same growth parameters as for the III-metal-polar AlGaN, but without using the low-temperature AlN nucleation layer. Since N-polar AlGaN films are usually rough, smooth N-polar GaN was grown using a 2° miscut (0001) sapphire to facilitate refractive index measurements.[28] A detailed description of the growth conditions for smooth N-polar AlGaN can be found elsewhere.[29] The composition of the AlGaN layers was determined by high-resolution x-ray diffraction in a triple axis geometry to determine the *c*-lattice parameter through the use of the (002) symmetric reflection and relating it to composition by using Vegard's law; it was assumed that the films were fully relaxed as expected from growth directly on a low-temperature AlN nucleation layer. Considering the maximum possible uncertainty in the strain state of the film, the maximum bound for the Al composition uncertainty is ±0.025 of the reported values.[28]

The prism coupling method was used to determine the refractive indices of the thin film waveguides.[30–32] A schematic drawing of the setup is displayed in Figure 1. It consisted of an excitation laser, a prism to couple the light in and out of the sample, and a detector to measure the reflected laser light. All measurements were performed at four different wavelengths: Ar^+ ion laser (457.9 nm), Nd:YAG laser (532 and 1064 nm), and HeNe laser (632.8 nm). A half-wave plate controlled the polarization of the incoming beam. A rutile prism was glued onto a custom made holder and the sample was pressed against the base of the prism. A converging lens focused the laser beam at the prism base. The reflected light was coupled out through the prism and directed onto a photodiode. The sample holder consisted of an *xyz* translator and a 3-axis angular stage, which enabled precise positioning of the focal point onto the prism base. The holder and the photodiode were mounted on two separate rotation stages with a common axis actuated by stepper motors with angular resolution better than 1 arcsec. The Sellmeier coefficients for the refractive indices of the prism were taken from the work of Rams *et al.*[33]

In this method, light is coupled into the waveguide under different angles of incidence and the intensity of the reflected light is measured. A strong coupling of the incident

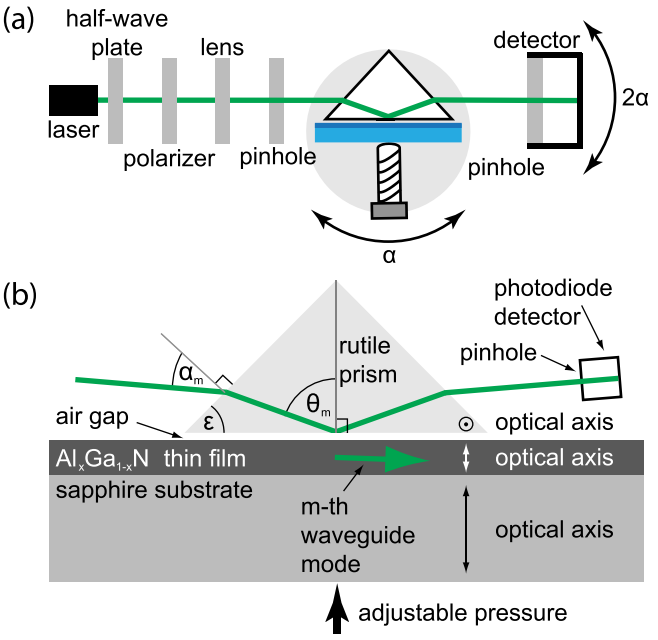

FIG. 1. Schematic of the prism-coupling set-up. (a) Polarization of the laser is adjusted and the beam is focused onto a prism base to a spot size of 50 μm. The reflected signal is measured by a photodiode; a pinhole is used to block the beams originating from internal reflections in the prism. (b) Enlarged view of the prism coupling setup to launch a single guided mode *m* into the AlGaN waveguide. The film, the sapphire substrate, and the rutile prism are optically uniaxial with the direction of the axes as marked in the figure. A symmetric rutile prism with an apex angle ε of 45.00° is used.

beam into the film occurs when the component of the impinging wave vector parallel to the layer surface meets the propagation constant of a distinct waveguide mode ($m = 0$, 1, 2,…), leading to a decrease of the intensity of the reflected light. The minima-positions in the reflected intensity depend on the waveguiding properties of the layer, allowing for simultaneous determination of the refractive index and thickness. In addition, by using both polarizations of the incoming light (TE: electric field polarized parallel to the film surface, TM: electric field polarized approximately normal to the film surface), birefringence of the film can be obtained if the film is thick enough to support at least two guided TE and TM modes.[16,30–32,34–37]

The prism coupling measurement technique is more precise than ellipsometry because it is only slightly affected by variations in the film refractive index or by optical absorption in the film, effects, which cause complications in ellipsometry measurements.[38] In our experience, it is also less sensitive to surface roughness. As described above, the films have to be thick enough to support at least two guided TE and TM modes.[16,30–32,34–37,39] In addition, the surface roughness must be well below the wavelength of the coupled light. The latter can be a problem especially for N-polar AlGaN since as-grown surfaces of this polarity are often covered by hillocks.[29,40] In order to overcome this problem, smooth N-polar GaN grown on 2° miscut sapphire was used. AFM measurements on these samples revealed a root-mean-square (RMS) surface roughness of about 1 nm, which is below the typical RMS values obtained from N-polar GaN layers grown on (0001) sapphire.[29] Figure 2 displays two typical AFM topographs of the III-polar and N-polar $Al_xGa_{1-x}N$

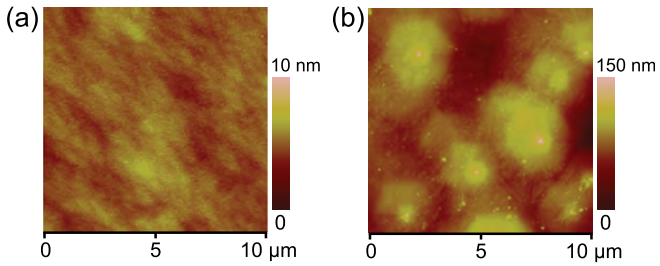

FIG. 2. Topographical AFM images of (a) III-metal-polar $Al_{0.025}Ga_{0.975}N$ and (b) N-polar $Al_{0.105}Ga_{0.895}N$ sample. Note the different height scales.

with x = 0.025 and x = 0.105, respectively. The surface of the III-polar AlGaN showed RMS roughness values below 5 nm, independent on the Al-content. In contrast, N-polar AlGaN was covered with pyramidal hillock structures (Figure 2(b)), the size of which decreased drastically with increasing Al-concentration leading to smooth N-polar surfaces even for AlGaN films with very low Al-content. This effect was attributed to a change in supersaturation due to the (tri)methyl aluminum flow leading to a change in the growth mode.[29,41] However, even for the rougher films the surface roughness was always well below the wavelength of the coupled light, allowing for effective application of the prism coupling method.

As mentioned above, a strong coupling occurred when the in-plane projection of the phase velocity of the incoming beam matched the phase velocity of an optical mode in the layer. In order to calculate the modes in our optical waveguide, a coordinate system with the *xy* plane parallel to the film surface was chosen. In this configuration the *z*-axis was perpendicular to the film surface, and thus, parallel to the *c*-axis of the film. The two families of modes that can propagate in such a planar waveguide are the transverse electric (TE, ordinary polarized) and transverse magnetic (TM, extraordinary polarized) modes. The two modes are described as follows:

$$\vec{E}(\vec{r}) = (0, E_y(z)e^{i(\beta x-\omega t)}, 0)\,, \tag{1}$$

$$\vec{H}(\vec{r}) = (0, H_y(z)e^{i(\beta x-\omega t)}, 0), \tag{2}$$

where $E_y(z)$ and $H_y(z)$ describe the transverse field distribution. The propagation constant $\beta = n_{\text{eff}}k_0$ is the *x* component of the wave vector, which can be expressed by n_{eff}, the effective refractive index, and $k_0 = 2\pi/\lambda$, the vacuum wave number where λ is the vacuum optical wavelength.[42] The propagation of the modes is described by the following equations:

$$\frac{\partial^2 E_y}{\partial z^2} + k_0^2(n_o^2 - n_{\text{eff}}^2)E_y = 0, \tag{3}$$

$$\frac{\partial^2 H_y}{\partial z^2} + k_0^2(n_e^2 - n_{\text{eff}}^2)H_y = 0, \tag{4}$$

where n_o and n_e are the ordinary and extraordinary refractive indices, respectively. The boundary conditions at the film-air and film-substrate interfaces for the electric and magnetic field in Eqs. (3) and (4) lead to transcendental equations. By solving the equations, a set of optical guided modes are found which propagate with $n_{\text{eff},m}$. An isotropic approximation was used for the boundary conditions for the TM modes, which sets the film and substrate refractive indices to their respective extraordinary refractive indices. The comparison with the analysis taking into account the full birefringence[35,39] will be discussed later.

The effective refractive indices of the guided modes are found by measuring the coupling angles through the Snell's relation

$$n_{\text{eff},m} = n_p \sin\theta_m, \tag{5}$$

where θ_m is the coupling angle and n_p is the prism refractive index. The most accurate way to determine the coupling angles is by measuring the intensity of the reflected beam. As described, the reflection decreases strongly at certain prism angles α_m. An example of a typical measurement is shown in Figure 3. The prism angles α_m are then transformed to coupling angles θ_m by taking into account the refraction on the prism surfaces. It should be mentioned that even though the coupling condition is optimized for a specific *m*-mode, also all the other modes are weakly excited due to optical scattering inside the film. These unwanted modes are subsequently also out-coupled at specific angles. This phenomenon can be observed on the screen as a pattern of bright discrete *m*-lines.[30]

A least square method was used to fit the effective refractive indices of the measured modes. In order to solve the transcendental equation numerically for each polarization (Eqs. (3) and (4)) with appropriate boundary conditions, at least two modes must be measured. This allows simultaneous calculation of the refractive index n_o or n_e, and the film thickness *w*. Depending on the wavelength, sample thickness, and surface quality, up to 10 modes were measured. The resolution of the simulation was 0.001 for refractive index and 1 nm for thickness.

The uncertainty in the measurements of the refractive indices for $Al_xGa_{1-x}N$ samples is influenced by the following factors. One is the uncertainty of the refractive index and the angles of the prism. Error of the refractive indices of the prism was taken from Rams *et al.*,[33] while our measurement of all three normal reflections of the prism showed uncertainty of the angles below 0.005°. Taking into account both uncertainties, the error of the measurement of one mode's propagation constant is below 0.1%. The precision of the refractive index of the waveguide obtained by fitting the propagation

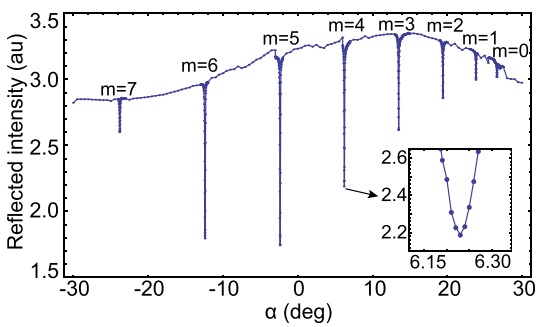

FIG. 3. Coupling curve for the III-metal-polar GaN sample at 532 nm for TE polarization. The sharp dips at the coupling angles indicate very high optical crystal quality. The angular resolution of the measurement around the coupling angles was 0.01°.

constants is significantly increasing with the number of measured modes. In Table I, the number of measured modes is presented for each sample and compared with the number of calculated modes. Based on our calculations the largest standard uncertainty for the refractive indices is ±0.1% for the case, where all existing modes were measured and used in fitting process, and increases to ±0.4% for the refractive indices obtained by fitting only two measured modes.

For N-polar samples with high aluminum content, the uncertainty is dominated by the surface roughness. The degree of film roughness affects mostly the results of the thickness and the refractive index results are less sensitive to it. Comparing the AFM images (Figure 2) with the inaccuracy in thickness (Table I), a high level of consistency can be observed. The uncertainty introduced by the sapphire refractive index data is negligible.[36,43]

As mentioned above, the isotropic approximation for the boundary conditions was used which simplifies the numerical calculations for TM modes. Following Sanford *et al.*[35] and Pezzagna *et al.*,[39] isotropic approximation can be used for the determination of the extraordinary refractive index and affects mostly the results on the film thickness. This was confirmed by our comparison of both methods for a few typical cases. The results for the extraordinary refractive indices obtained by both methods vary from sample to sample but never exceed 0.3%. As Sanford *et al.*[35] report we also see larger differences in n_e values for the samples, where fewer modes were measured. Number of measured modes was lower for the TM polarization (Table II) mostly due to a lower ordinary refractive index of the prism, thus the error on n_e is larger compared to the n_o measurements. Therefore, we estimate that the error of the n_e introduced by isotropic approximation is less significant than the error produced by a limited number of the measured modes. We also observed that values of film thickness obtained by TM polarization measurement are in average smaller for 10–20 nm in comparison to the ones from TE polarization measurements, which is consistent with the Sanford *et al.*[35] observation. Full birefringence method would then bring better results on the film thickness but we have to take into account that N-polar films are relatively rough; therefore, the error due to the film roughness is dominant.

TABLE I. The number of modes observed at particular wavelength and polarization compared to the number of calculated modes at given wavelength, refractive indices, and film thickness. The samples 1-5 are III-metal-polar and the samples 6-9 are N-polar. In case where all existing modes were measured the largest standard uncertainty for the refractive indices is ±0.1% and increases to ±0.4% for the refractive indices obtained by fitting only two measured modes.

		458 nm		532 nm		633 nm		1064 nm	
Sample		TE	TM	TE	TM	TE	TM	TE	TM
1	GaN	8/9	4/9	8/8	5/8	6/6	3/6	3/4	3/4
2	$Al_{0.025}Ga_{0.975}N$	6/10	6/10	7/8	4/8	6/7	3/7	3/4	2/4
3	$Al_{0.110}Ga_{0.890}N$	5/10	6/10	6/8	5/8	6/7	3/7	4/4	2/4
4	$Al_{0.170}Ga_{0.830}N$	7/9	6/9	7/8	5/8	5/6	3/6	4/4	2/4
5	$Al_{0.260}Ga_{0.740}N$	5/8	5/8	7/7	5/7	6/6	4/6	3/3	2/4
6	GaN	7/10	5/10	8/8	4/8	7/7	3/7	4/4	2/4
7	$Al_{0.025}Ga_{0.975}N$	6/7	4/7	6/6	4/6	5/6	3/5	3/3	2/3
8	$Al_{0.105}Ga_{0.895}N$	6/7	4/7	5/6	4/6	5/5	3/5	3/3	2/3
9	$Al_{0.300}Ga_{0.700}N$	8/8	5/8	7/7	4/7	5/6	4/6	2/3	1/3

TABLE II. Thickness and refractive indices obtained by prism coupling. Refractive indices are described by the Sellmeier coefficients from Eqs. (6) and (7). The samples 1-5 are III-metal-polar and the samples 6-9 are N-polar. Due to large degree of roughness for sample 8, coefficients for the extraordinary refractive index could not be obtained.

Sample	$Al_xGa_{1-x}N$	Thickness (nm)	A_{TE}	B_{TE} (nm)	A_{TM}	B_{TM} (nm)
1	GaN	1213 ± 12	4.180	182.8	4.300	195.42
2	$Al_{0.025}Ga_{0.975}N$	1296 ± 14	4.132	180.7	4.279	188.64
3	$Al_{0.110}Ga_{0.890}N$	1365 ± 9	4.054	174.2	4.204	182.22
4	$Al_{0.170}Ga_{0.830}N$	1282 ± 9	3.990	170.3	4.136	179.21
5	$Al_{0.260}Ga_{0.740}N$	1182 ± 11	3.913	161.7	4.039	174.26
6	GaN	1324 ± 20	4.116	189.9	4.200	204.18
7	$Al_{0.025}Ga_{0.975}N$	952 ± 32	4.072	183.2	4.198	188.54
8	$Al_{0.105}Ga_{0.895}N$	942 ± 32	4.056	179.4	…	…
9	$Al_{0.300}Ga_{0.700}N$	1112 ± 69	3.889	164.4	4.015	176.45

The ordinary and extraordinary indices measured at various wavelengths were fitted using first-order Sellmeier dispersion formula

$$n_o^2 = 1 + \frac{A_{TE}\lambda^2}{\lambda^2 - B_{TE}^2}, \tag{6}$$

$$n_e^2 = 1 + \frac{A_{TM}\lambda^2}{\lambda^2 - B_{TM}^2}. \tag{7}$$

The fitted values are given in Table II and the Sellmeier curves are shown in Figure 4. The fitted curves and the data points agree well, which indicates that the first-order Sellmeier formula is sufficient in the measured wavelength range.

Refractive index results obtained in this study for III-metal polarity are in good agreement with works like Özgür *et al.*,[34] Sanford *et al.*,[35] and Tisch *et al.*[44] For example, a comparison with the values provided by Sanford *et al.* shows that the largest difference in refractive index is 0.5%, but for most of the data points it is below 0.1%. However, all these works

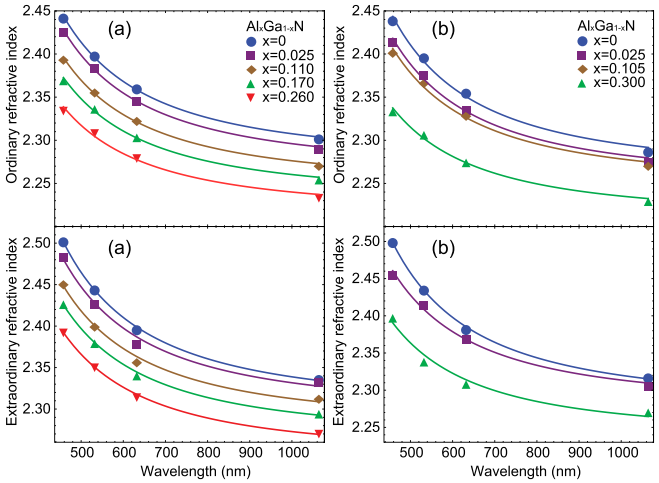

FIG. 4. Wavelength dependence of ordinary and extraordinary refractive indices for AlGaN with different Al-concentration. (a) III-metal-polar samples, (b) N-polar samples. Symbols represent prism coupling measurements at discrete wavelengths and the curves are first-order Sellmeier fits.

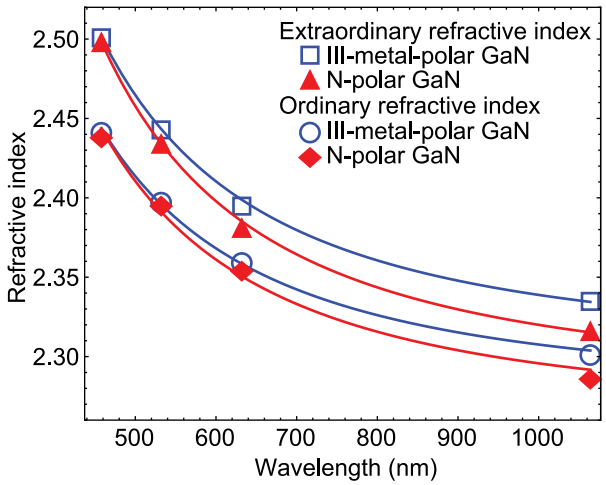

FIG. 5. Comparison of ordinary and extraordinary refractive indices between GaN samples of both polarities. Symbols represent prism coupling measurements at discrete wavelengths, curves are first-order Sellmeier curves.

only investigated the III-polar AlGaN layers. In contrast, in this work the refractive indices of the N-polar AlGaN thin films were also measured. As an example, the refractive indices of GaN over the whole investigated wavelength regime for both polarities are displayed in Figure 5. A comparison between the samples of both polarities shows that the N-polar samples have a slightly lower refractive index. It can be seen that the difference is more pronounced at longer wavelengths. In case of the GaN films, the difference in the ordinary refractive index is 0.1% at 457.9 nm and increases to about 0.6% at 1064 nm. Even though the uncertainty in the refractive index measurements is larger for the N-polar than for III-polar films, the uncertainty is still smaller than the measured refractive index difference between both polarities. The refractive index should not change by a 180° rotation of the crystal, so the smaller refractive index of N-polar samples throughout the whole region of wavelengths is most likely due to the different incorporation of unwanted impurities during growth for the two polarities; it is known that the oxygen impurity concentration is about two orders of magnitude higher in the N-polar material.[45] However, further investigations are needed to clarify this observation.

In summary, we have measured and compared the refractive indices for both, III-metal-polar and N-polar, $Al_xGa_{1-x}N$ thin films grown by MOCVD on sapphire substrate. The dispersion of ordinary and extraordinary refractive indices was measured at four wavelengths between 458 and 1064 nm in samples with the Al concentration x up to 0.30. The dispersion was described well by the first-order Sellmeier equation. In addition, a small difference in refractive indices between the two materials with different polarity was observed, which probably arose due to different impurity levels in films of different polarity.

The NCSU group acknowledges a partial financial support by the Army Research Laboratory, Contract No.: W911NF-04-D-0003, William Clark program monitor and NSF under Contract DMR-1108071.

[1]A. J. Fischer *et al.*, Appl. Phys. Lett. **84**, 3394 (2004).
[2]J. P. Zhang *et al.*, Appl. Phys. Lett. **81**, 4910 (2002).
[3]T. Nishida *et al.*, Appl. Phys. Lett. **79**, 711 (2001).
[4]Y. Taniyasu, M. Kasu, and T. Makimoto, Nature **441**, 325 (2006).
[5]M. Kneissl *et al.*, J. Appl. Phys. **101**, 123103 (2007).
[6]H. Yoshida *et al.*, New J. Phys. **11**, 125013 (2009).
[7]C. Rhodes, IEEE J. Quantum Electron. **10**, 153 (1974).
[8]S. Nakamura, S. Pearton, and G. Fasol, *The Blue Laser Diode*, 2nd ed. (Springer Verlag, Berlin, 2000).
[9]H. Morkoc, *Nitride Semiconductors and Devices* (Springer, New York, 1999).
[10]R. Collazo *et al.*, Phys. Status Solidi A **207**, 45 (2010).
[11]S.-R. Jeon *et al.*, Appl. Phys. Lett. **86**, 082107 (2005).
[12]R. Dalmau *et al.*, J. Electrochem. Soc. **158**, H530 (2011).
[13]J. Xie *et al.*, Phys. Status Solidi C **8**, 2407 (2011).
[14]J. L. P. Hughes *et al.*, Phys. Rev. B **55**, 13630 (1997).
[15]N. A. Sanford *et al.*, J. Appl. Phys. **97**, 053512 (2005).
[16]H. Y. Zhang *et al.*, Appl. Phys. Lett. **69**, 2953 (1996).
[17]Y. Fujii *et al.*, Appl. Phys. Lett. **31**, 815 (1977).
[18]A. Yariv, *Optical Electronics in Modern Communications*, 5th ed. (Oxford University Press, New York, 2003).
[19]J. Lin and H. Jiang, in Conference on Lasers and Electro-Optics (CLEO), Baltimore, MD, 22–27 May 2005.
[20]S. Wang *et al.*, Opt. Lett. **24**, 978–980 (1999).
[21]A. Chowdhury *et al.*, Appl. Phys. Lett. **83**, 1077 (2003).
[22]J. Miragliotta *et al.*, J. Opt. Soc. Am. B **10**, 1447–1456 (1993).
[23]S. D. Hum and M. M. Fejer, C. R. Phys. **8**, 180–198 (2007).
[24]R. Katayama *et al.*, Proc. SPIE **8268**, 826814 (2012).
[25]R. Collazo *et al.*, Appl. Phys. Lett. **91**, 212103 (2007).
[26]N. A. Fichtenbaum *et al.*, J. Cryst. Growth **310**, 1124 (2008).
[27]M. P. Hoffman *et al.*, Proc. SPIE **8631**, 86311T (2013).
[28]R. Kirste *et al.*, J. Appl. Phys. **110**, 093503 (2011).
[29]S. Mita *et al.*, Phys. Status Solidi C **8**, 2078 (2011).
[30]R. Ulrich and R. Torge, Appl. Opt. **12**, 2901–2908 (1973).
[31]P. K. Tien, Appl. Phys. Lett. **14**, 291 (1969).
[32]E. Dogheche, B. Belgacem, D. Remiens, P. Ruterana, and F. Omnes, in *GaN and Related Alloys - 1999*, edited by H. Amano, R. Feenstra, T. Myers, and M. S. Shur (MRS, 1999).
[33]J. Rams *et al.*, J. Appl. Phys. **82**, 994 (1997).
[34]U. Özgür *et al.*, Appl. Phys. Lett. **79**, 4103 (2001).
[35]N. A. Sanford *et al.*, J. Appl. Phys. **94**, 2980 (2003).
[36]M. J. Bergmann *et al.*, Appl. Phys. Lett. **75**, 67 (1999).
[37]G. M. Laws *et al.*, J. Appl. Phys. **89**, 1108 (2001).
[38]A. C. Adams *et al.*, J. Electrochem. Soc. **126**, 1539 (1979).
[39]S. Pezzagna *et al.*, J. Appl. Phys. **103**, 123112 (2008).
[40]M. Stutzmann *et al.*, Phys. Status Solidi B **228**, 505 (2001).
[41]S. Mita *et al.*, J. Appl. Phys. **104**, 013521 (2008).
[42]K. Kawano and T. Kitoh, *Introduction to Optical Waveguide Analysis: Solving Maxwell's Equation and the Schrodinger Equation* (Wiley-Interscience, New York, 2001).
[43]W. J. Tropf and M. E. Thomas, *Handbook of Optical Constants of Solids III* (Academic, San Diego, 1998).
[44]U. Tisch *et al.*, J. Appl. Phys. **89**, 2676 (2001).
[45]T. K. Zywietz *et al.*, Appl. Phys. Lett. **74**, 1695 (1999).